

# Electrochemical characterization of passivated electrogalvanized steel

Célia R. Tomachuk<sup>1</sup>, Cecilia I. Elsner<sup>2</sup>, Alejandro R. Di Sarli<sup>2</sup>

<sup>1</sup> Centro de Ciencia e Tecnologia de Materiais do Instituto de Pesquisas Energéticas e Nucleares, IPEN/CCTM, Av. Prof. Lineu Prestes, 2242, 05508-000, Sao Paulo, SP, Brazil, tomazuk@gmail.com

<sup>2</sup> CIDEPIINT: Research and Development Centre in Paint Technology (CICPBA-CONICET LA PLATA); Av. 52 s/n entre 121 y 122. CP. B1900AYB, La Plata-Argentina

## Introduction

The chromate conversion treatment is widely used, but it requires highly toxic chromic acid solutions, with consequent effluent disposal and ecological problems [1-5]. The removal of these toxic chemicals is considered a priority within European Union. In this work, the corrosion resistance behavior of three alternative pretreatments applied on electrogalvanized steel was investigated by electrochemical techniques. Their results were compared with those obtained for traditional Cr<sup>6+</sup>-based pretreatment exposed to the same conditions. The experiments were carried out in aerated 0.3 M Na<sub>2</sub>SO<sub>4</sub> solution, pH 10, at 25 °C. From the analyses and interpretation of the attained data could be inferred that the alternative coatings systems exhibited discrete protective properties in aerated alkaline sulfate solution. The nitro-cobalt chemical conversion treatment showed protective properties like the traditional Cr<sup>6+</sup>-based one, while the Cr<sup>3+</sup>-based pretreatment displayed a very poor anticorrosive performance, and the phosphate one initially provided good protective action but this decreased as the time elapsed. The EIS technique proved to be able for distinguishing between the protective properties afforded by each pretreatment exposed to an alkaline media.

## Experimental

Electrogalvanized steel samples (7.5 cm x 10 cm) industrially produced and covered with the following conversion treatments: **(A)** Cr<sup>+3</sup> chromate; **(B)** nitro-cobalt chemical conversion; **(C)** phosphate; and **(D)** traditional Cr<sup>6+</sup> chromate, were investigated.

For each conversion layer, an individual commercial conversion bath was formulated and the coating was produced according to the recommendations of the respective supplier.

Coatings thickness was measured using the Helmut Fischer equipment DUALSCOPE MP4.

Coatings morphology was observed by scanning electron microscopy (SEM), while the surface microanalysis was performed by energy dispersive spectrometry (EDS), using a LEICA S440 microscopic.

Electrochemical impedance measurements were performed in the frequency range between 10<sup>-2</sup> Hz a 10<sup>5</sup> Hz using a Solartron 1260 Frequency Response Analyzer coupled to a Solartron 1286 electrochemical interface, and a sinusoidal voltage signal of 3 mV. The corrosion behavior was analyzed till the appearance of white corrosion products on the samples surface. All measurements were performed at a constant room temperature of 25°C in aerated 0.3 M Na<sub>2</sub>SO<sub>4</sub> solution, pH 10, in which the zinc dissolution rate is very slow [6]. Test electrolytes were prepared from analytical grade materials and distilled water. Solution pH was adjusted by small additions of NaOH solution.

The electrochemical cell consisted of a PMMA cylindrical electrolyte holder attached to the coated surface filled with the test solution. The exposed area was 7.07 cm<sup>2</sup>. Coated metal was the working electrode. A reference electrode Hg/HgSO<sub>4</sub> (SSE) and a Pt counter electrode were employed. Throughout the paper, all the electrochemical potentials are referred to the Saturated Calomel Electrode (SCE).

## Results and Discussion

The thickness and composition of the investigated samples are reported in Table 1. As can be observed, the coatings thickness was uniform through the entire surface. Samples with **A**, **C** and **D** treatments were lucid grey, while **B** treatment had dark grey coloration. In all these

treatments it was not possible to obtain information about the passive layer thickness. Table 1 shows the total thickness of the coating (zinc plus passive layer).

Table 1: Thickness and composition of zinc coatings after conversion treatment

Identification of samples	Conversion treatments based on	Composition	Coatings thickness ( $\mu\text{m}$ )
A	$\text{Cr}^{3+}$	Zn, Fe, Cr, P, S	9.1
B	Nitro-cobalt	Zn, Fe, Co, P, S	9.7
C	phosphate	Zn, Fe, P, S	9.5
D	$\text{Cr}^{6+}$	Zn, Fe, Cr, P, S	8.7

Coatings surface morphology was observed by SEM at 2.000X and 10.000X enlargement, Fig. 1. **A** treatment presented a less uniform structure formed by smaller nodular grains. At lower magnifications, the **B** treatment exhibited small spherical shaped particles distributed over the surface, which have a strong tendency to agglomerate forming filaments. The surface morphology of **C** and **D** treatments was very similar and exhibited a plate-like structure. The **D** treatment showed a more uniform and compact structure.

The EDS semi-qualitative element analysis of the surface coatings revealed the presence of S and P; probably related to the sulfate and phosphate ions coming from the treatment baths. The **A** and **D** treatments did not present the typical network of cracks, characteristic of chromated coatings, probably due to the low treatment thickness. The coatings exhibited uniform, micro-rough and homogenous structure with irregular size growth.

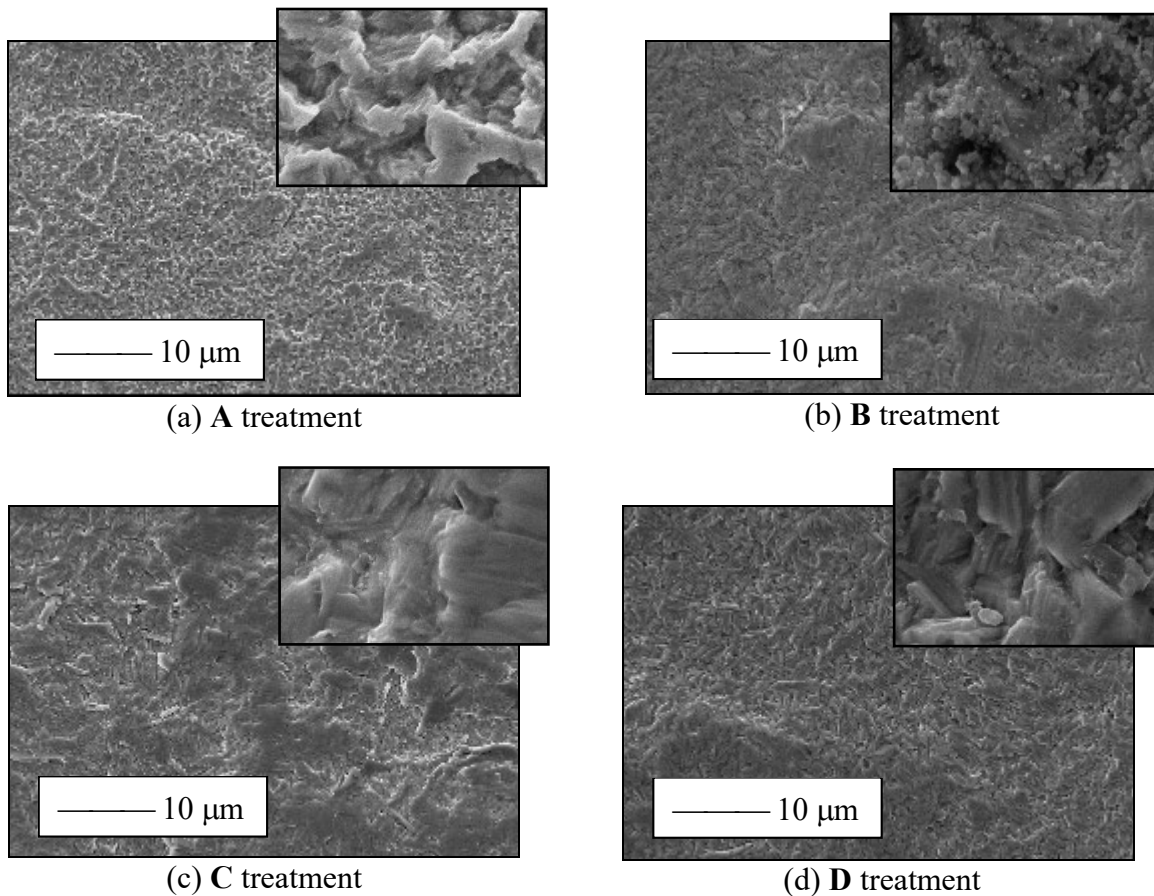


Fig. 1: SEM micrographs of the electrogalvanized steel samples covered with different conversion treatments.

Impedance spectra – EIS measurements were carried out at ambient temperature and concluded upon observation of the macroscopic appearance of white corrosion products [7].

Figure 2(a) shows the Bode plot of impedance modules as a function of the immersion time in the test solution for **A** treatment. It is observed that, at the lower frequency (0.02 Hz), the  $|Z|$  magnitude tended to increase slightly as the time elapsed up to reach values near to  $2.10^3 \Omega \cdot \text{cm}^2$ . After 24h of immersion, at medium frequencies was observed a decrease of  $|Z|$ , that is, an increase of the capacitance value. At high frequencies, the  $|Z|$  values are related to the corrosion resistance of the conversion coating and, as they did not change during the immersion period, it suggests that the surface remained unchanged during this period.

Figure 2(b) shows phase angle shift as a function of immersion time in the test solution for the **A** treatment. It is observed a time constant with a maximum phase angle value of  $58^\circ$ , and also that, at 0.02 Hz, the phase angle curve slope suggests the appearance of a second time constant. After 2h of immersion and, at medium frequencies, it is observed a small variation of this time constant and its disappearance after 24h of immersion. A possible justification of such behavior is based on the assumption that the conversion coating is not compact. So, initially, the surface corrosion protection took place through the gathering of corrosion products within and/or at the bottom of the coating pores, but as the time elapsed that protection is lost because the products diffused towards the bulk of the solution.

Figure 2(c) shows the Bode plot of impedance modules as a function of immersion time in the test solution for the **B** treatment. At the lower frequency (0.02 Hz) was observed an oscillating behavior during the immersion time. It was attributed to the existence of a corrosion reaction at the interface, in agreement with the variation of the potential values. At high frequency was observed an increase of the  $|Z|$  value after 24 h of immersion, which suggests a compaction of the corrosion products within and/or at the bottom of the coating pores causing an inhibition of the corrosion process.

Figure 2(d) shows the phase angle evolution as a function of the immersion time in the test solution for the **B** treatment. Initially, only one time constant associated to the presence of the treatment film and with a maximum phase angle of  $55^\circ$  was observed but, after 50 min, a second time constant appeared indicating that the corrosion of the substrate surface had started. After 24 h, the second time constant disappeared, possibly due to the coatings defects were blocked by the corrosion products developed and, consequently, the corrosion process was inhibited.

Figure 2(e) shows the Bode plot of impedance modules as a function of immersion time in the test solution for **C** treatment. At 0.02 Hz, an oscillating behavior during the first hour was detected, being the initial  $|Z|$  value equal to  $2.10^4 \Omega \cdot \text{cm}^2$ . After the first hour, the  $|Z|$  values tended to decrease as a function of immersion time. At high frequency, an increase of  $|Z|$  with the immersion time was observed, which suggests an improvement on the coating protective properties, but this improvement was not enough to prevent the corrosion of the substrate during larger immersion periods. This type of behavior can be explained assuming that the developed corrosion products were able to block the coatings defects sufficiently as to inhibit, at least partially and temporarily, the occurrence of the substrate corrosion reactions.

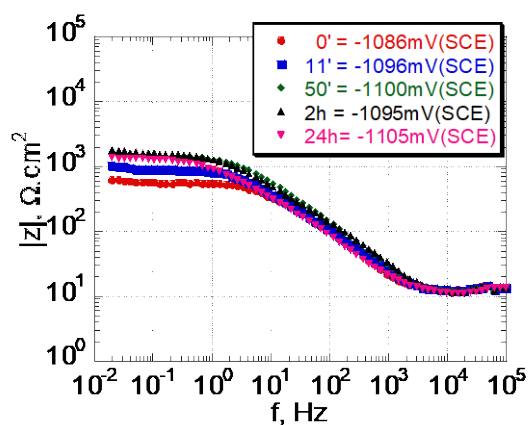
Figure 2(f) shows phase angle shift as a function of immersion time in the test solution for the **C** treatment. For the first 2h immersion at least two time constants were well defined. The high frequency one was associated to the presence of the treatment film, while the observed at the low frequency range was associated to the zinc corrosion reaction. After 24h, a third time constant appeared at medium frequencies and this was interpreted as an evidence of the corrosion products contribution to the overall system impedance.

Figure 2(g) shows the Bode plot of impedance modules as a function of immersion time in the test solution for the **D** treatment. At low frequency (0.02 Hz), an slightly oscillating behavior of the  $|Z|$ , with an initial value of  $5.10^3 \Omega \cdot \text{cm}^2$ , was observed. At high frequencies can be noted that the conversion coating initially offers a corrosion protection due to the gathering of corrosion products within and/or at the bottom of the coating pores, but after 24h of

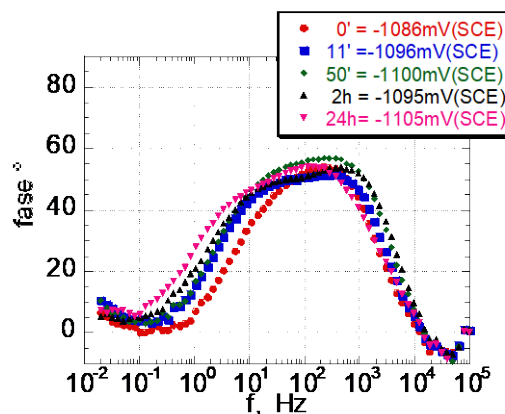
immersion the  $|Z|$  value went back to its initial value. This means that after the initial protection offered by the corrosion products, a more significant degradation of the conversion layer took place. Changes happening in the conversion layer have highly detrimental effects on the corrosion behavior of the coated steel.

Figure 2(h) shows phase angle shift as a function of immersion time in the test solution for the **D** treatment. It can be seen that the time constant at low frequencies, and present just after immersion ( $t = 0$ ), disappeared after 25 min of immersion and it was substituted by an inductive loop. At medium frequencies there was a phase angle maximum of  $75^\circ$ . A second time constant did not appear which means that the slight modifications occurred in the conversion layer did not affect the behavior of the total coating.

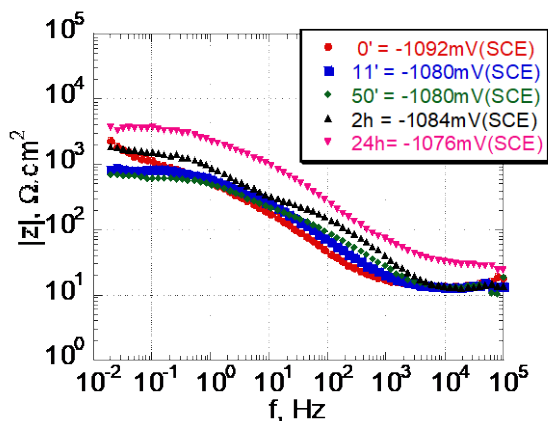
A qualitative analysis of the EIS data shows that the **C** and **A** treatments suffered degradation and corrosion at the metal/conversion layer interface during the exposure to the alkaline solution, while **D** and **B** treatments remained more or less unchanged and showed the best performance. Thus, the deterioration with the conventional  $\text{Cr}^{6+}$ -based treatment was lower than that of the tested alternative conversion treatments; probably due to its layer was structurally and morphologically more uniform and compact than others ones.



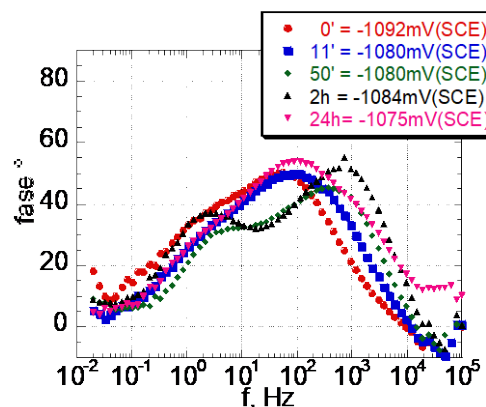
(a) Bode – treatment A



(b) phase angle – treatment A



(c) Bode – treatment B



(d) phase angle – treatment B

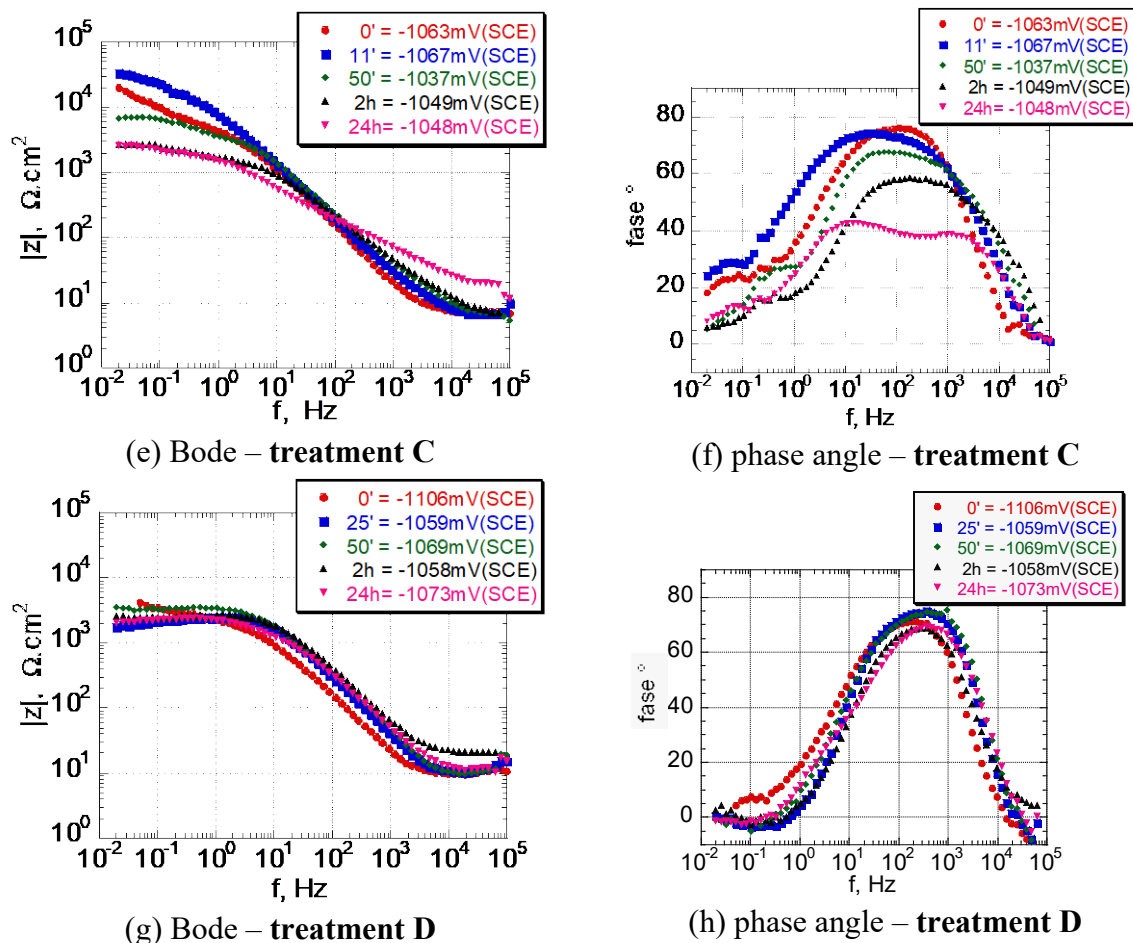


Fig. 2. Bode and phase angle plots as a function of immersion time in aerated 0.3 M Na<sub>2</sub>SO<sub>4</sub>.

## Conclusions

The development of the present experimental study allows the following main conclusions to be drawn:

- all treatments presented white corrosion products after 24 h of immersion in 0.3 M Na<sub>2</sub>SO<sub>4</sub> solution at pH 10;
- the EIS data showed the different coatings corrosion behavior in the initial stage of the immersion, but after 2h of immersion was difficult to observe such difference, probably due to the formation of corrosion products, not visible by the naked eye;
- EIS data demonstrated that the **D** treatment shoed good corrosion protection, which was comparable to the **B** treatment, and that the **A** treatment provided the poorer protective properties;
- Initially, the **C** treatment showed good anticorrosive protection but this decreased as the exposure time elapsed.
- the more uniform and compact coating presented the best corrosion behavior;

## Acknowledgements

This research was financed by the European Commission under contract ERK6-CT1999-0009, and Comisión de Investigaciones Científicas de la Provincia de Buenos Aires (CICPBA), Consejo Nacional de Investigaciones Científicas y Técnicas (CONICET) and Universidad Nacional de La Plata (UNLP) of Argentina.

## References

1. P.L. Hagans, C.M. Hass, ASM Handbook Surface Engineering. 5 (1994) 405.
2. A. Barbucci, M. Deluchi, G. Cerisola. Prog. Org. Coat., 33 (1998) 131.
3. C.R. Tomachuk, C.I. Elsner, A.R. Di Sarli, O.B. Ferraz. Mat. Chem. Physics, 119 (2010) 19.

4. C.R. Tomachuk, C.I. Elsner, A.R. Di Sarli. *Mat. Sci. Appl.*, 01 (2010) 202.
5. C.R. Tomachuk, F.M. Queiroz, I. Costa *ECS Trans (online)*, 43 (2012) 45.
6. J. Hazan, C. Coddet, M. Keddam, *Corr. Sci.*, 31 (1990) 313.
7. J.R. Mac Donald. *Impedance Spectroscopy Emphazing Solid State Materials*. Ed. J. Miley & Sons, N.Y. (1987).